Journal of Zhejiang University-SCIENCE A (Applied Physics & Engineering)
ISSN 1673-565X (Print); ISSN 1862-1775 (Online)
www.jzus.zju.edu.cn; www.springerlink.com
E-mail: jzus@zju.edu.cn

Wind suitability in site analysis of coastal concave terrains using computational fluid dynamics simulation: a case study in East Asia*

Xiao-qing ZHU[†1,2], Jian-tao WENG[3], Yi-qun WU[3], Wei-jun GAO[2], Zhu WANG[3]

([1]*Urban Planning and Habitation Construction Research Center, Zhejiang University of Technology, Hangzhou 310014, China*)

([2]*Faculty of Environmental Engineering, University of Kitakyushu, Kitakyushu 802-8577, Japan*)

([3]*Department of Architecture, Zhejiang University, Hangzhou 310058, China*)

[†]E-mail: arc_zxq@163.com

Received Apr. 15, 2016; Revision accepted Nov. 9, 2016; Crosschecked Aug. 15, 2017

Abstract: The effect of wind environment is becoming increasingly important in analyzing and selecting sites for better natural ventilation of residential buildings, external comfort, and pollution dispersion. The main purpose of this study was to develop a set of methods for wind environment assessment in coastal concave terrains. This set of methods can be used to provide quantifiable indicators of preferable wind conditions and help site analysis. Firstly, a total of 20 types of coastal bays with concave terrains in East Asia were characterized to find ideal locations. The selected areas were divided into five categories according to the main terrain features. Then a sample database for the concave terrains was compiled for modelling comparisons. Secondly, a number of key wind variables were identified. Computational fluid dynamics (CFD) models of the typical coastal concave terrains identified as a result of the study were created, and the local wind environments were simulated with input from geographic information system (GIS) and statistic package for social science (SPSS) analysis. A measure of wind suitability was proposed that takes wind velocity and wind direction into account using GIS. Finally, SPSS was used to find the relationship between wind suitability and key terrain factors. The results showed that wind suitability was significantly associated with terrain factors, especially altitude. The results suggest that residential building sites should be selected such that their bay openings face the direction of the prevailing wind and that the opposite direction should be avoided.

Key words: Wind suitability; Residential building; Computational fluid dynamics (CFD); Coastal concave terrains; East Asia
http://dx.doi.org/10.1631/jzus.A1600313 **CLC number:** TU023

1 Introduction

Historically, concave bays were preferable residential building sites for human settlement in coastal areas because of their obvious geographical benefits. The terrain conditions are characterized by a concave surface: a plain with one side open to the beach and the rest surrounded by low hills. In East Asia, since coastal land is limited and demand has increased recently due to rapid economic growth, land use has been continuously optimized and adjusted. Effective land use has now gradually become one of the major objectives in coastal construction and sustainable development. Analysis and selection of residential sites play an important part at the preliminary design stage. In line with the rapid growth of urbanization and population in coastal areas, the quality of residential building sites has become a major concern, especially its impact on external comfort, building thermal performance, natural ventilation, pollution dispersion in urban design, and master planning. As for the wind environment, reports of several typhoon disasters in recent years have shown that the degree of

* Project supported by the National Natural Science Foundation of China (Nos. 51208466 and 51238011), the Science and Technology Research Program of Chinese Ministry of Housing and Urban-Rural Development (No. 2014R2-036), the Humanities and Social Sciences Research Foundation of the Ministry of Education (No. 17YJAZH136), the Natural Science Foundation of Zhejiang Province (No. LY16E0 80011), and the Social Sciences Planning Project of Zhejiang Province (No. 12JCSH02YB), China

ORCID: Xiao-qing ZHU, http://orcid.org/0000-0002-0786-2944

© Zhejiang University and Springer-Verlag GmbH Germany 2017

damage in villages and small towns in coastal areas was directly related to features of the terrain. Therefore, it is necessary to assess the regularity of the wind environment in complex terrains and provide a basis for site selection for residential buildings, to enhance natural ventilation and pollution dispersion in the planning and design stage.

The wind environment in coastal concave terrains is complex and quite different from that in open plains. In particular, wind fields close to the ground are unevenly distributed over the complex terrain surface within a mesoscale region. The measured data from local weather stations can provide only a limited range for reference. Therefore, there is a need to obtain high-resolution wind field data about the surface layer of complex terrains. These data will then provide quantifiable information for assessment of residential building sites and for masterplan design.

At present, in addition to simple desk-top wind analysis, two main methods are used in wind simulation studies: wind tunnel testing and computational fluid dynamics (CFD). Wind tunnel testing is a conventional, well-established, and reliable method that has been used in a lot of studies. Because wind tunnel tests are inefficient and time-consuming, most researchers have focused on single cases. For example, Takahashi *et al*. (2002) explained the turbulence characteristics of 2D mountain boundaries based on a wind tunnel testing method. Bowen and Hong (1992) investigated the characteristics of peak-gust windspeeds taken from wind tests based on a smooth isolated hill. Bullard *et al*. (2000) studied the influence of different attack angles on wind fields in mountainous terrains. McAuliffe and Larose (2012) developed a terraced-model approach for measuring the wind characteristics over a complex terrain. Not only should the scale of the turbulence length of the inflow be large and typical, but also concave terrains are quite big and complex, so in many cases it is difficult to determine the characteristics of the wind field. Kubota *et al*. (2008) took 22 real cases in Japan as examples and revealed the relationship between the building density and wind velocity at pedestrian level by wind tunnel tests. However, these cases were located in plain areas. Wind conditions in concave terrains influenced by terrain fluctuation and the direction of opening are very different from those of plain areas. As pointed out by Chock and Cochran (2005), due to limitations in the size of wind tunnel tests and the model scale, it is difficult to produce a reliable wind field test for big and complex terrains. Moreover, a wind tunnel test has a long cycle and is quite expensive. Therefore, numerical simulation is the method of choice for wind environment evaluation on mesoscopic scales, providing sufficient details of the air movement near the ground surface or at pedestrian level.

Due to great improvements in hardware and the development of computational technology, CFD simulation is now widely used in wind field research and commercial design for its advantages of efficiency, convenience, and high level of detail. Taylor *et al*. (1986) first put forward simple guidelines for estimating wind velocity variation in complex terrains. Weng *et al*. (2000) then focused on the effects of small-scale terrain features and proposed new formulations based on results of calculated flow over hills. Due to restrictions on model geometry and experimental techniques, most studies on numerical simulation of wind fields in specific complex terrains have focused on targeted analysis of some specific examples. Tang *et al*. (2012) carried out a quantitative investigation of Shang-gan-tang village in China by adopting CFD simulation, to explore the design concepts of traditional settlements and the residential building site. Lei *et al*. (2013) proposed a method to simulate the detailed wind field around buildings over complex terrains, taking the Hong Kong International Airport during Typhoon Nuri as an example. Li *et al*. (2007) presented a numerical and experimental study of wind modelling over a domain that contained both porous and bluff objects. Their models can simulate wind conditions in an urban outdoor open space, including windbreaks and buildings. This showed that CFD modelling can be used as a tool to assess the sheltering effects of windbreaks in master planning and landscape design for a better outdoor environment. Hu and Wang (2005) discussed the requirement for accuracy when using CFD in a built-up area. Their study suggested that applying a CFD approach was effective for investigating street-level winds if the grid density and turbulence models were correct. Sugimura *et al*. (2009) calculated wind flow using a mesoscale meteorological model and showed that most conditions of the wind flow variation were similar to experimental conditions. In terms of residential

buildings, many researchers have used CFD to optimize layouts so that they have a suitable wind environment. Ramponi *et al*. (2015) presented CFD simulations of outdoor ventilation for generic configurations with different urban densities and street widths. The results showed that the effect of a main street on outdoor ventilation depended on the wind direction. However, there are no systematic rules for residential building site analysis based on the wind environment in coastal concave terrains. Most existing quantitative measurements of wind environments provide methods only for the effective use of wind energy (Takahashi *et al*., 2005). Such research results cannot be regarded as direct references for construction.

The geographic information system (GIS) has been widely applied in data preparation and analysis for planning. Kumar and Bansal (2016) provided a GIS-based methodology to locate a safe site, considering many spatial safety aspects. Latinopoulos and Kechagia (2015) used GIS as a decision tool for wind-farm site planning. GIS has proved useful for retrieving information from a mess database and can assist planners and engineers in determining the best site for buildings.

This study aimed to develop a method of wind assessment for site analysis specifically for concave terrain conditions in coastal areas. This method consists of CFD wind modelling, GIS spatial analysis, and the introduction of a quantifiable indicator for East Asia. A measure of wind suitability is proposed that takes wind velocity and direction into account. A model is established to assess wind suitability in coastal concave terrains, wind distribution rules are analyzed according to terrain features, and recommendations are made for wind environment analysis.

2 Coastal concave terrains

2.1 Background

In most coastal concave terrains, a settlement is normally located on the north side, facing south. The mountain can slow down the chilly winds from the north in winter. The residents welcome a gentle breeze from the southeast in summer. This overall pattern of village form is suggested by "Fengshui" (Fig. 1), the indigenous science for human settlements in China (Mak and Ng, 2005). In such a village, buildings support each other because of narrow foundations. They represent an organic free-style layout. The buildings in this area show mainly a clumped distribution. The major roads tend to follow the coastline and those linking buildings throughout the settlement. Village development in coastal areas of East Asia has a long history. In general, their layout and architectural form reflect the local lifestyle, and aesthetic trend varies from one village to another. The site selection, layout, and scale of the village are in line with the principle of adapting to local conditions. In the coastal areas of East Asia, settlement development was slow and any problems that arose could be corrected gradually over time. However, the modern construction pattern is quite rapid and a high quality of living quality is demanded, including natural ventilation of individual buildings, a masterplan for external comfort, pollution dispersion, and the use of wind loading calculations in structural design. Thus, it is necessary to assess the outdoor wind environment.

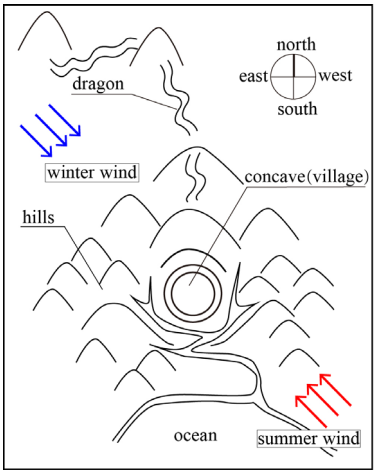

Fig. 1 A schematic diagram of the "Fengshui" model of a coastal concave terrain. Modified from (Mak and Ng, 2005)

2.2 Classification of coastal concave terrains

To maintain the consistency of the climatic conditions in research samples, the scope of this study was restricted to the coastal areas of East Asia (119.1°–133.5° E, 23.5°–35.0° N) in the subtropical monsoon climate zone (Fig. 2). In general, the prevailing winds are from the sea to the southeast in summer, and from the northwest in winter. According to the direction of the opening of coastal concave

terrains, a total of 20 sampling sites were selected and divided into five categories: down-crosswind, windward, up-crosswind, leeward, and crisscross. Their characteristics are listed in Table 1 according to their statistical classification and distribution. Fig. 3 shows the terrain details of the 20 selected sites. The sites were all coastal concave terrains, in which mountains and hills covered more than 75% of the total land.

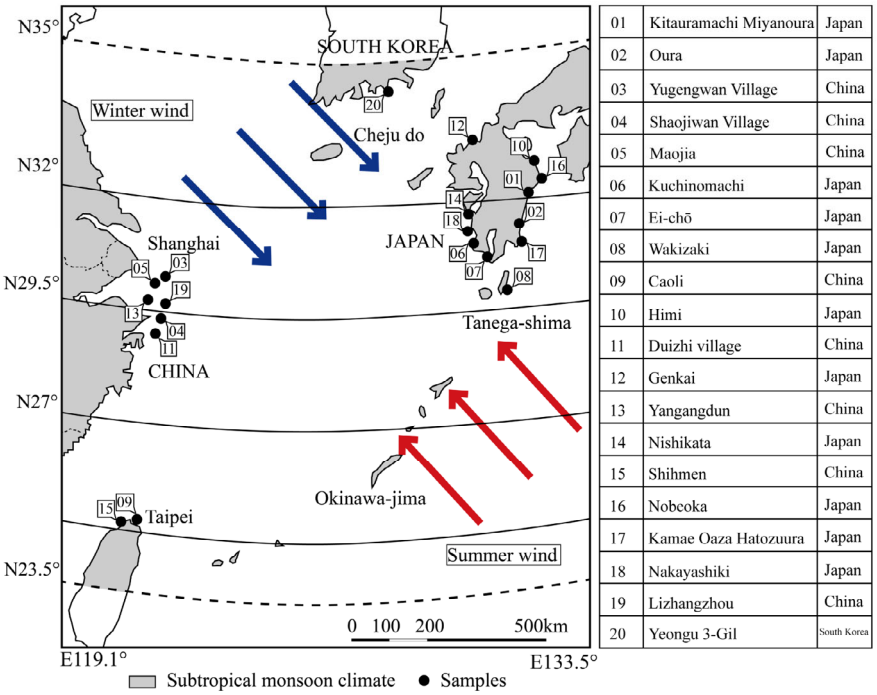

01	Kitauramachi Miyanoura	Japan
02	Oura	Japan
03	Yugengwan Village	China
04	Shaojiwan Village	China
05	Maojia	China
06	Kuchinomachi	Japan
07	Ei-chō	Japan
08	Wakizaki	Japan
09	Caoli	China
10	Himi	Japan
11	Duizhi village	China
12	Genkai	Japan
13	Yangangdun	China
14	Nishikata	Japan
15	Shihmen	China
16	Nobcoka	Japan
17	Kamae Oaza Hatozuura	Japan
18	Nakayashiki	Japan
19	Lizhangzhou	China
20	Yeongu 3-Gil	South Korea

Fig. 2 Cases of coastal concave terrains in East Asia

Table 1 Classification of the coastal concave terrains

Item	Type I	Type II	Type III	Type IV	Type V
Description	Down-crosswind	Windward	Up-crosswind	Leeward	Crisscross
Diagram	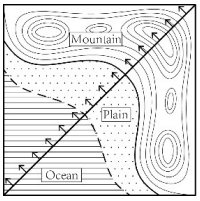	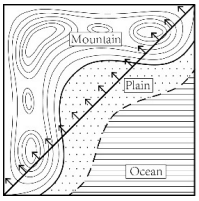	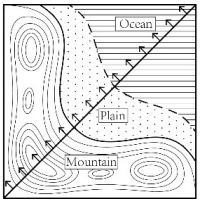	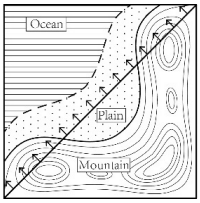	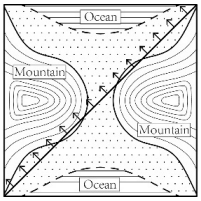
Configuration with typical characteristics	Openings of coastal concave terrains are perpendicular to the wind direction; open to the southwest	Openings of coastal concave terrains are parallel to the wind direction; open to the southeast	Openings of coastal concave terrains are perpendicular to the wind direction; open to the northeast	Openings of coastal concave terrains are parallel to the wind direction; open to the northwest	Openings of coastal concave terrains cross the wind direction; open to the northsouth direction
Location	Located mainly in the southwest corner of coastal islands	Located mainly in the southeast corner of coastal islands	Located mainly in the northeast corner of coastal islands	Located mainly in the northwest corner of coastal islands	Located mainly in the northwest corner of coastal islands
Selected sampling sites	Kitauramachi Miyanoura, Japan; Oura, Japan; Yugengwan Village, China; Shaojiwan Village, China	Maojia, China; Kuchinomachi, Japan; Ei-chō, Japan; Wakizaki, Japan	Caoli, China; Himi, Japan; Duizhi village, China; Genkai, Japan	Yangangdun, China; Nishikata, Japan; Shihmen, China; Nobeoka, Japan	Kamae Oaza Hatozuura, Japan; Nakayashiki, Japan; Lizhangzhou, China; Yeongu 3-Gil, South Korea

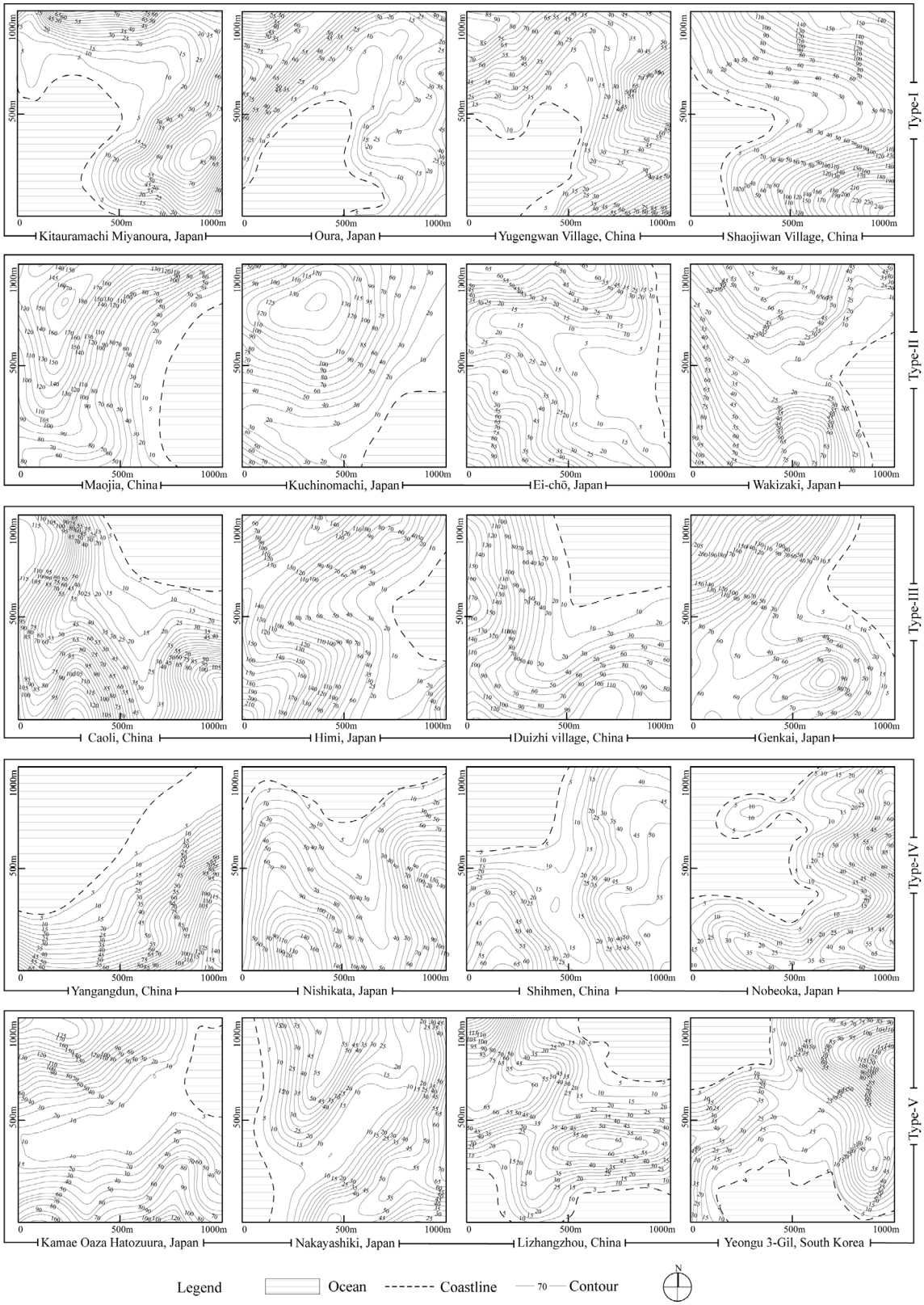

Fig. 3 Cases of coastal concave terrains in East Asia

3 Model for evaluation of wind suitability in site analysis

3.1 CFD simulation

A total of 20 kinds of typical cases (Fig. 3) were chosen as the objects. FLUENT was used for developing a wind simulation model. CFD grids with high precision were required to generate simulated wind fields in coastal concave terrains. High-precision terrain elevation data were obtained from ASTER GDEM, based on the latitude and longitude of measuring points used for validation. Since the ASTER GDEM data downloaded from the National Aeronautics and Space Administration (NASA) were part of a geographic coordinate system based on WGS84, coordinates for the projection were converted into Universal Transverse Mercator (UTM) to simplify the calculation. The terrain network was quickly formed following the method of Cheng and Fei (2006). The buildings and trees were not considered. The size of models in the study was set as 1000 m×1000 m×Z (X×Y×Z), where Z was the highest altitude of mountains in each sample, which was considered sufficient to minimize the boundary effects in the computation. Considering the limits of simulation accuracy, an unstructured tetrahedral mesh system known as the Kitauramachi Miyanoura configuration was used in this wind model. The computational domain was 3000 m×3000 m×300 m (Fig. 4a). Three different grid sizes were used to find a reasonable grid.

According to Table 2, a grid size of 226×10^3 is reasonable (Fig. 4b). A grid size of 226×10^3 can meet the requirements of grid independence and ensure the efficiency of calculation.

3.1.1 Turbulence model

Non-linear models that solve the Navier-Stokes equations numerically have the advantage of being able to simulate complex problems, compared with linear models (Yan and Li, 2016). Reynolds average Navier-Stokes (RANS) models, the most popular non-linear models, have been shown to perform reasonably well when applied to wind prediction over complex terrains (Castro *et al*., 2003; Vuorinen *et al*., 2015). Recently, the large-eddy simulation method has been used to simulate the wind fields over complex terrain. However, its implementation incurs massive computational demands and takes a long time. In this study, 3D steady and incompressible RANS models were applied. The influence of the Coriolis term was neglected (Mellor and Yamada, 1982), since the horizontal scale of the simulation

Table 2 Grid independence examination

Number of grids ($\times10^3$)	Average wind velocity at 1.5 m (m/s)	Relative error rate of wind velocity	Average wind direction at 1.5 m (radian)	Relative error rate of wind direction
113	7.19	–	0.71	–
226	7.35	2.23%	0.72	4.23%
450	7.39	2.78%	0.75	5.62%

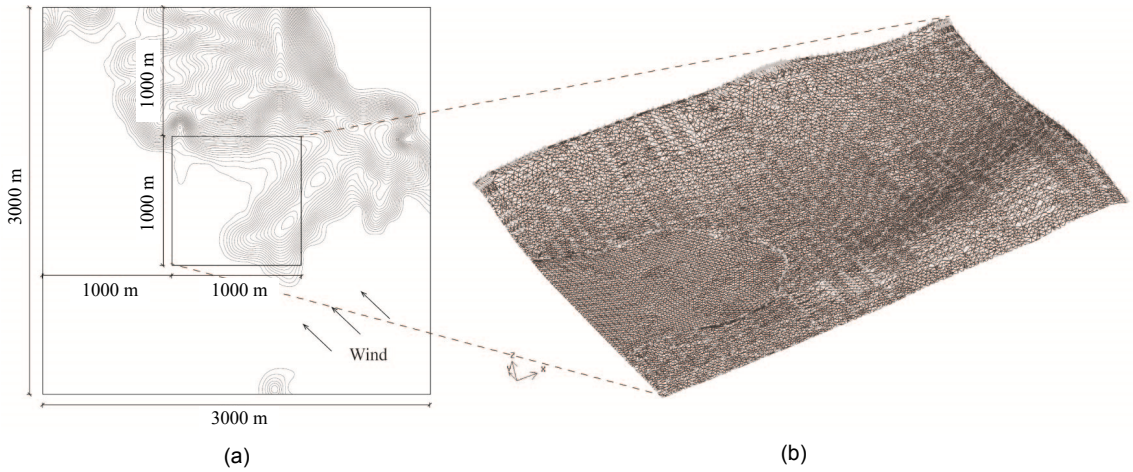

Fig. 4 Mesh configuration of Kitauramachi Miyanoura, Japan
(a) Computational domain; (b) Close-up view of a grid in the study area

range was no more than 10 km. The standard k-ε model developed by Launder and Sharma (1974) was used. Researchers have proved that this model can help produce a reliable result (Liu *et al*., 2010).

3.1.2 Boundary conditions

In this case, the computational domain was large and the side boundaries were far away from the surface of the concave terrains. The profiles were set according to user-defined functions (UDFs), using FLUENT 2009. The approved velocity profile was used as follows:

$$U_z = \frac{U_0}{k} \ln\left(\frac{z + z_0}{z_0}\right), \tag{1}$$

where z is the distance from the ground level, U_z is the instantaneous resolved velocity, U_0 is the friction velocity, z_0 is the roughness length, and k is the von Kármán constant (0.42), according to the FLUENT manual.

3.1.3 Modelling wind conditions

As winter winds are the subject of a future study, here we focus on the natural ventilation quality in summer. This simulation took summer as the main evaluation season for investigating external comfort, pollutant diffusion, and natural ventilation conditions in these regions. The wind in the final simulated conditions was set as the prevailing wind in each case. According to the local weather bureaus and climate data from www.energyplus.com, the average reference speed in all cases in summer was about 5.5 m/s. Therefore, this value was adopted for all cases. Finally, wind fields in each case were solved by CFD simulation for wind assessment in built wind environments (Fig. 5).

3.2 Influencing factors

As climatic conditions determine the wind strength and direction, evaluation factors at the measuring points include the wind velocity and wind direction. Wind has a great effect on human thermal comfort through its influence on both latent and sensible heat exchange (Szűcs, 2013), and also affects the thermal performance of buildings.

The wind velocity (V) and wind direction (D) were normalized to dimensionless variables to be used as rating indicators of the wind conditions for comprehensive site analysis. Many methods are used to evaluate wind environments, including the Beaufort Wind Scale (Meaden *et al*., 2007), Oliver Wind Effect Index and Davenport Criterion (Murakami *et al*., 1986). Considering the operability of this study and with reference to the studies of Penwarden (1973), Wise and Richards (1971), and Murakami and Deguchi (1981), we set a mean wind speed of 5 m/s as the upper limit of wind environment comfort. Since a wind velocity greater than 10 m/s will seriously influence the movement of pedestrians (Simiu and Scanlan, 1978), it was set as the threshold of danger. Furthermore, to ensure the effectiveness of natural ventilation within the settlement, the wind velocity needs to be greater than 1.5 m/s (MHURD, 2014). Based on these reviews, a new scoring criterion was proposed according to comfort and safety (Table 3, p.749).

Wind direction directly affects the efficiency of natural ventilation, which is determined by the angle between the wind direction at measuring points and the best orientation of buildings. $\Delta\varphi$ is the projecting angle of wind against buildings (Fig. 6, p.749). Ecotect software was used to analyze and calculate the best orientation of buildings in each case. The calculation was based on the local solar radiation in extremely hot and cold periods of the year. The best orientation is a compromise between less solar radiation during extremely hot days and more solar radiation during extremely cold days. Since wind directions at measuring points cannot be directly measured, they were obtained by the calculation of wind velocity components in the X and Y axes of the simulated measuring points V_x and V_y (Fig. 7, p.749).

$$\theta = \arctan(V_y / V_x), \tag{2}$$

$$\Delta\varphi = \left|\pi / 2 - \theta - \varphi\right|, \tag{3}$$

where V_x is the wind velocity component in the X axis, V_y is the wind velocity component in the Y axis, θ is the wind direction at the measuring points, and φ is the best orientation of buildings in a certain region.

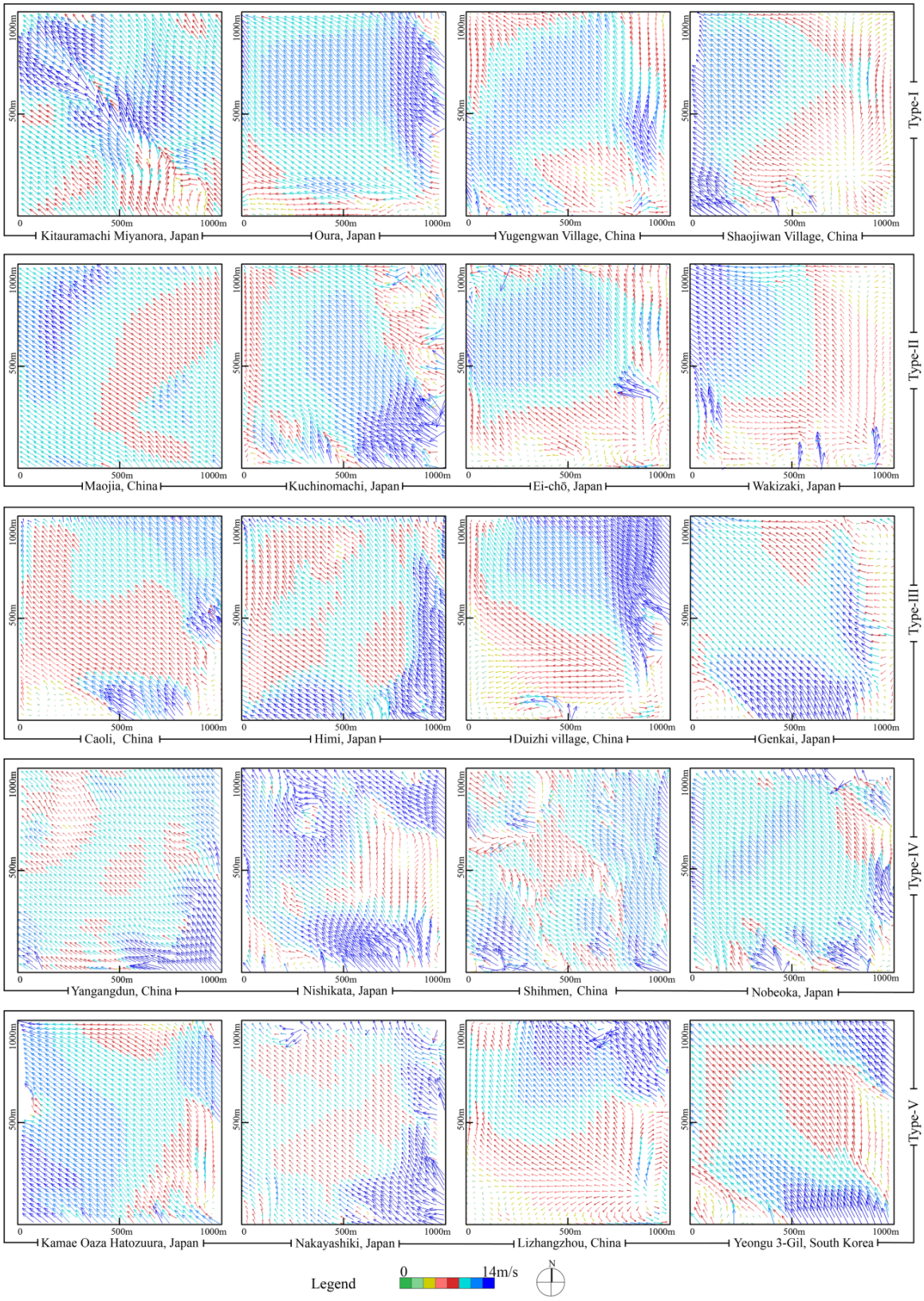

Fig. 5 CFD results of coastal concave terrains at the pedestrian level

Finally, we took the induced angle ($\Delta\varphi$) between wind directions at measuring points and the best orientations as the basis of assessment. Both the wind velocity and induced angle were divided into six levels (Table 3). Each data point contained information about wind velocity and wind direction. For example, φ in Fig. 7 represents the best orientation of buildings in a certain region. Classification grids of polar coordinates were drawn according to the categories in Table 3. Next, the locations of data at the measuring points were determined with polar coordinates. For instance, (ρ_1, θ_1) is the polar representation of A, ρ_1 represents the wind velocity at point A, and θ_1 is calculated by Eq. (2).

3.3 Wind suitability for site analysis

To effectively assess the external comfort and natural ventilation of wind environments, the two non-dimensional variables, wind velocity and wind direction, were integrated to form a new dimensionless parameter named wind suitability (WS):

$$\mathrm{WS}=\mathrm{INT}\left(\sqrt{(V'^2+D'^2)/2}\right), \tag{4}$$

where V' is the classification value of wind velocity and D' is the classification value of wind direction. According to the value of wind suitability, the sample rating was divided into six levels. Based on the classifying criteria of wind energy resources presented by Noorollahi *et al*. (2016), wind suitability was graded into suitability classes 1 to 6, in order of increasing suitability. Areas of wind suitability in classes 5 and 6 were considered preferable and those in classes 1 or 2 were considered undesirable.

3.4 Output of wind suitability

To explain the characteristics of complex terrains clearly, according to Tamura (1969; 1983)'s classification of landforms and the specificity of coastal terrain topology, we roughly divided the coastal concave terrains into a crest slope, upper side slope, head hollow, lower slope, foot slope, and plain (Dai and Miura, 1997). A 3D model of a typical

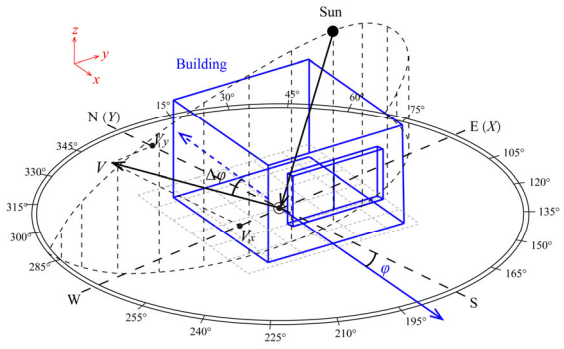

Fig. 6 Isometric diagram of a wind measuring point

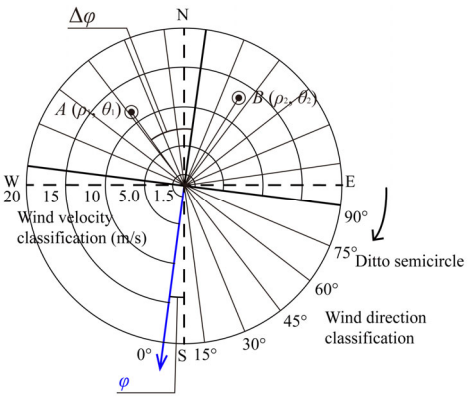

Fig. 7 Polar coordinates of a wind measuring point

Table 3 Wind velocity and wind direction classification

Wind velocity classification			Wind direction classification		
Velocity (m/s)	Description of comfort and safety	V'	Induced angle	Description of natural ventilation	D'
$V\leq1.5$	Calm	5	$\Delta\varphi\leq15°$	Well ventilated from south to north	6
$1.5<V\leq5$	Comfortable	6	$15°<\Delta\varphi\leq30°$	Ventilation effects are not bad	5
$5<V\leq10$	Discomfort, moving is difficult	4	$30°<\Delta\varphi\leq45°$	Wind velocity is significantly weakened, creating turbulence	4
$10<V\leq15$	Unpleasant, seriously influencing movement	3	$45°<\Delta\varphi\leq60°$	Poor ventilation. Calm zone occurs	3
$15<V\leq20$	Hard to walk	2	$60°<\Delta\varphi\leq75°$	Ventilation is blocked	2
$V>20$	Dangerous	1	$75°<\Delta\varphi\leq90°$	No effective ventilation	1

coastal concave terrain is shown in Fig. 8. The data analyzed by CFD (Fig. 9) were imported into the ArcGIS platform. After the process of "Spatial Analyst Tools/Reclassify" in ArcGIS, wind velocity and wind direction data were reclassified and assigned values in accordance with Table 3. We adopted "Raster Calculator" in the module of "Spatial Analyst Tools" to calculate the wind suitability according to Eq. (4). Finally, we superposed digital elevation models (DEMs) in the GIS platform and divided the coastal concave terrains into six rating levels in accordance with the evaluation model of the wind suitability of site analysis. Fig. 10 shows the classification map of wind suitability in a typical concave terrain.

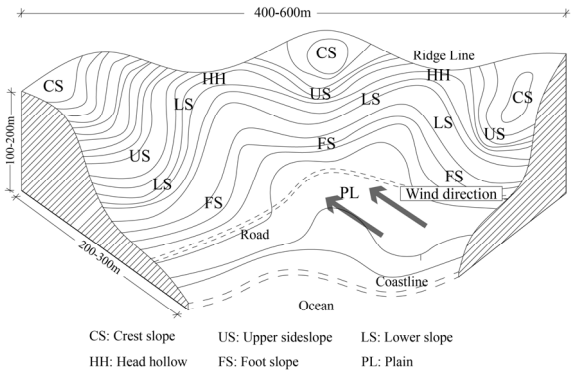

Fig. 8 3D model of typical concave terrains

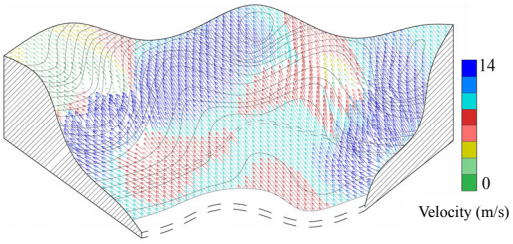

Fig. 9 CFD model of typical concave terrains

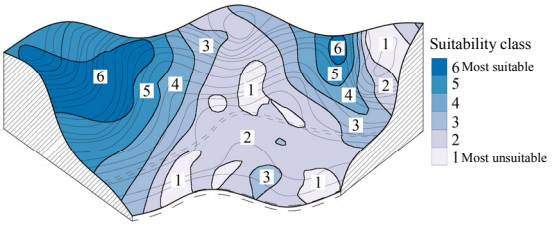

Fig. 10 Suitability class results of typical concave terrains

4 Results of wind suitability

After simulating typical cases, an evaluation chart of wind suitability could be obtained. The wind suitability results (Fig. 11) indicated that the coastal concave terrains could directly influence the layout of wind fields. Wind fields close to the ground within the simulation range were characterized by high unevenness. They were significantly influenced by terrain fluctuations. Moreover, the wind direction changed dramatically in mountainous terrains. The optimal locations for settlements in the coastal concave terrains in Fig. 10 are mainly on windward slopes. Since the crest of the hill was greatly influenced by the increase in wind velocity and slope gradient, it was not the most ideal choice. The ventilation effects in foothills were not bad. Due to protection by the windward slope, wind velocity in the leeward slope decreased. The wind velocity distribution was consistent before the wind reached coastal concave terrains, and the wind velocity varied within a small range. When the wind reaches the windward upper side slope, the wind velocity increases. Buildings could achieve the best wind environment if they were located on the windward slopes. In these areas, the wind suitability was the highest.

The CFD results from 20 cases showed that leeward slopes perpendicular to the wind direction were unsuitable for residential use since they were in a calm zone, which was bad for indoor air ventilation.

Compared to separate evaluation of wind direction and velocity, evaluation coupling the two can more intuitively reveal the advantages and disadvantages of wind environments in coastal concave terrains. According to the group comparison in Fig. 12 (p.752), the average value of wind suitability was the highest for type II, with a maximum value of 5.2, followed by type III (4.5) and type I (4.4). The worst types were type IV (3.5) and type V (3.0). Comparative results of the average wind suitability in different areas (Fig. 12) were as follows: windward> up-crosswind=down-crosswind>leeward>crisscross. In conclusion, we recommend the selection of terrains whose openings face the direction of the wind, and the avoidance of terrains whose openings are opposite to the wind direction.

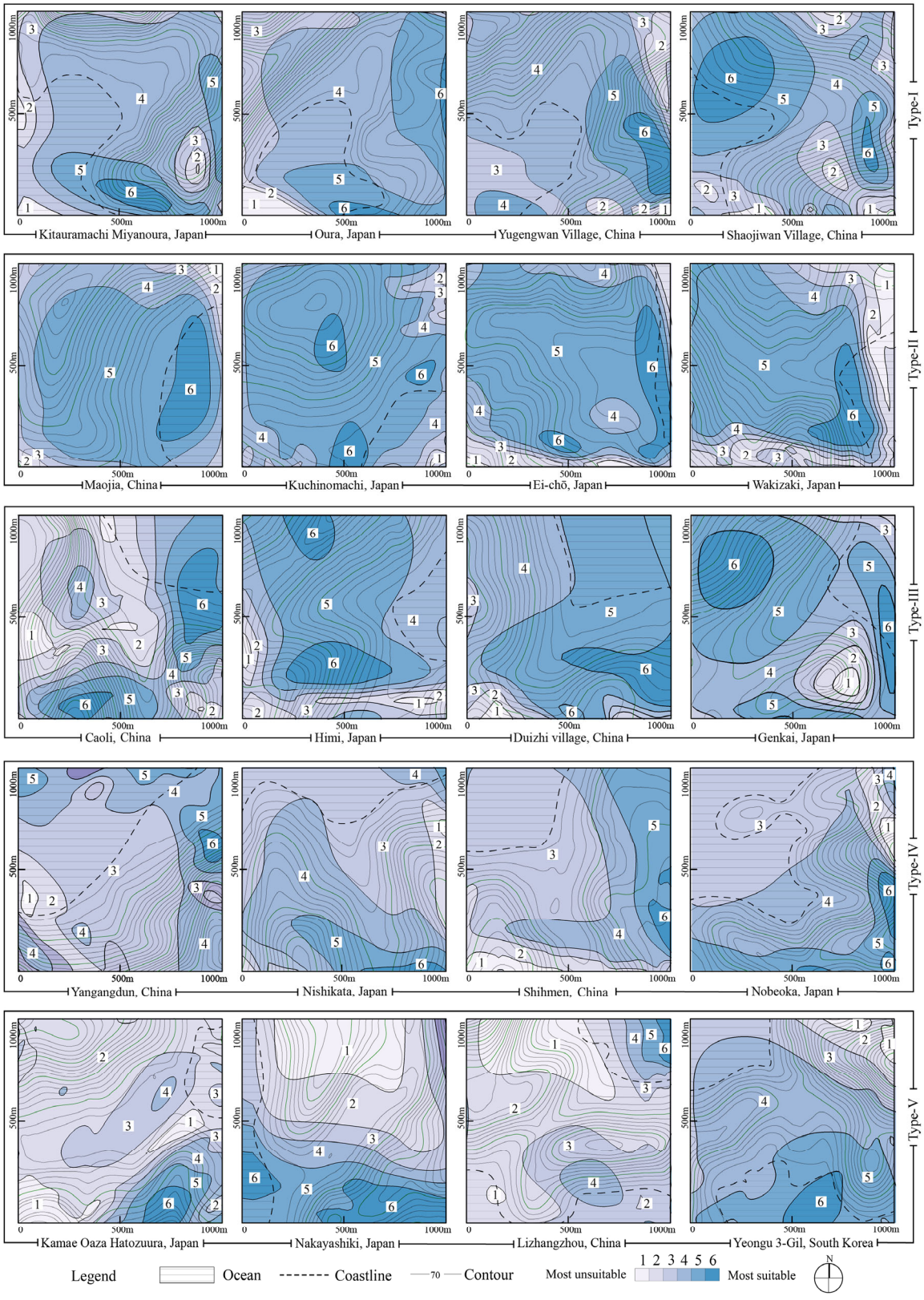

Fig. 11 Results of wind suitability from 20 samples

5 Discussion

5.1 Correlation with terrain factors

Altitude, slope gradient, and slope direction are the three main numerical variables representing terrain characteristics. Based on the cases, DEMs were used to generate spatial distribution maps of these three numerical variables, using "3D Analyst", "Spatial Analyst", and "Patch Analyst" modules in the GIS platform. The linear regression model is one of the most common statistical analysis methods used in this study.

Forty measuring points in each case were chosen at random. Since wind suitability is a categorical variable, the Spearman correlation method was selected in this study. The correlation analysis module of SPSS was adopted to analyze the correlation between wind suitability and altitude, slope gradient and slope direction. The significance (Sig.) of correlations between these variables is shown in Table 4. A Sig. (2-tailed) of less than 0.05 was taken as indicating a significant correlation between two factors. Correlation coefficients of less than 0 indicate negative correlations.

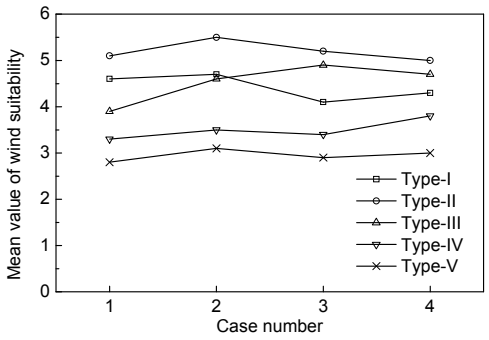

Fig. 12 Mean value of wind suitability in each type of terrain

The correlation between wind suitability and altitude was the most significant, with a correlation coefficient of −0.968. So altitude was the main terrain factor determining wind suitability. The correlation coefficient between wind suitability and slope gradient was −0.435, implying that the slope gradient was the second most important terrain factor. However, no correlation between slope direction and wind suitability was found, because the Sig. (2-tailed) was more than 0.05.

5.2 Wind suitability distribution comparison

In terms of guidelines for wind environments, it is important to grasp the characteristics of the distribution. A total of 40 measuring points where wind suitability was 5 or 6 were selected at random from within the area.

Classification standards for the three numerical variables were as follows: altitude, 0–10 m, 10–20 m, 20–30 m, 30–40 m, 40–50 m, 50–60 m, 60–70 m, 70–80 m, 80–90 m, and >90 m; slope gradient, 0°–10°, 10°–20°, 20°–30°, 30°–40°, 40°–50°, and 50°–90°; slope direction, the north direction was taken as 0° and the clockwise direction as positive direction. Slope directions were divided into eight equal parts.

Frequency distributions of altitude, slope gradient, and slope direction are shown in Figs. 13–15, respectively, according to different types. In Fig. 13, types I, II, and III showed a similar pattern in the distribution of altitude. A peak appeared at 0–10 m in types I, II, and III, and at 40–50 m in types IV and V. As for the slope gradient (Fig. 14), the five types were divided into two kinds of tendencies. The main concentration of the area suitable for construction was in the 20°–30° slope gradient in types I, II, and III, but steeper in types IV and V. The area suitable for

Table 4 Correlations analysis between wind suitability and terrain factors

Terrain factor	Slope gradient		Slope direction		Altitude		Wind suitability	
	Correlation coefficient	Sig. (2-tailed)	Correlation coefficient	Sig. (2-tailed)	Correlation coefficient	Sig. (2-tailed)	Correlation coefficient	Sig. (2-tailed)
Slope gradient	1.000	–	−0.057	0.001	0.458	0	−0.435	0
Slope direction	−0.057	0.001	1.000	–	−0.001	0.937	−0.011	0.520
Altitude	0.458	0	−0.001	0.937	1.000	–	−0.968	0
Wind suitability	−0.435	0	−0.011	0.520	−0.968	0	1.000	–

Correlations of <0.05 (2-tailed) are considered statistically significant; there are 800 measuring points

construction tended to be in a slope direction of 90°–180° in types I and II, and 225°–315° in types III, IV, and V (Fig. 15).

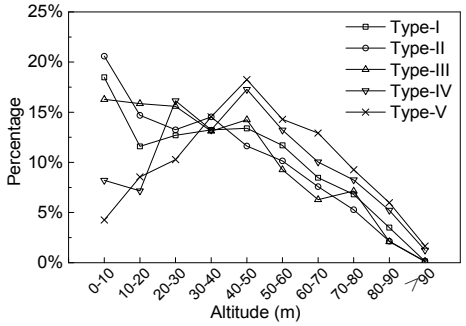

Fig. 13 Probability distribution of altitude

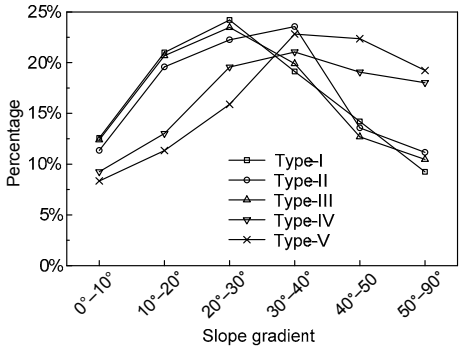

Fig. 14 Probability distribution of slope gradient

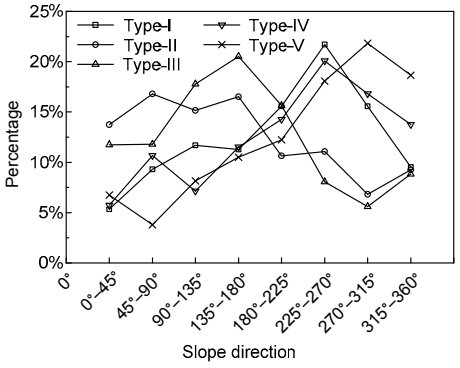

Fig. 15 Probability distribution of slope direction

5.3 Logistic regression analysis

To simplify the conclusion further, the probabilities of preferable and undesirable wind conditions were estimated to give a brief evaluation of the wind environment. We used a logistic regression model to simplify our models by reducing the number of dependent variables, and used a total of 800 measuring points in all cases selected above, so as to avoid spatial autocorrelation. We defined wind suitability classes 5 and 6 as having preferable wind conditions. Wind suitability classes 1 and 2 were considered to have undesirable wind conditions. The binary logistic regression of SPSS 20.0 was used for analysis to produce a mathematical model to predict the possibility of preferable wind conditions. The formulas are as follows:

$$\ln\left[P/(1-P)\right] = A_0 + A_1x_1 + A_2x_2 + \cdots + A_nx_n, \tag{5}$$

$$P = 1/\left[1+\exp(-z)\right], \tag{6}$$

$$z = A_0 + A_1x_1 + A_2x_2 + \cdots + A_nx_n, \tag{7}$$

where x_1, x_2, ..., x_n are independent variables, and A_1, A_2, ..., A_n are logistic regression coefficients. We took the natural logarithm ln[P/(1−P)] for P/(1−P), i.e., we performed logistic conversion. Therefore, the value range of the logistic was (−∞, +∞). This enabled the establishment of regression equations with the prediction probability P as the dependent variable.

Assume that P_p is the probability of preferable wind conditions and that P_i is the probability of undesirable wind conditions. In this study, after the calculation of SPSS, we obtained the logistic regression model of preferable wind conditions deduced from SPSS analysis as follows:

$$P_p = 1/\left[\exp(-1363.64 + 0.87x_1 + 0.41x_2 + 33.92x_3)\right], \tag{8}$$

where x_1 is the value of the slope gradient, x_2 is the value of the slope direction, and x_3 is the value of the altitude. SPSS results showed that the P value of samples was <0.05 and the Chi-square value was 5100.613. This indicated that the difference was significant. Moreover, the model passed the test. According to Eq. (8), the closer that the value P is to 1, the more likely is the measuring point to be in preferable wind conditions. Corresponding to the wind suitability shown graphically in Fig. 11, the total correct rate of fitting of Eq. (8) was 79.59%. Therefore, Eq. (8) can help to estimate roughly the probability of preferable wind conditions in this area.

The logistic regression model of undesirable wind conditions was deduced from SPSS analysis as follows:

$$P_i = 1/\left[1+\exp(897.25-0.87x_1-0.54x_2-26.89x_3)\right]. \quad (9)$$

SPSS results showed that the P value of samples was <0.05 and the Chi-square value was 4859.02. This indicated that the difference was significant. Moreover, the model passed the test. Corresponding to the wind suitability shown graphically in Fig. 11, the total correct rate of fitting Eq. (9) was 75.88%.

We used the data of the 20 cases to check the formulas, and the total correct rate of fitting was above 75%. Therefore, Eqs. (8) and (9) can provide a rough probability of preferable and undesirable wind conditions in the area. If detailed results are needed, we recommend using the evaluation model for wind suitability. The characteristics of different coastal concave terrains have been discussed and basic advice given. In future work, we will add more real examples to increase the accuracy of the empirical formula and make more specific recommendations.

6 Conclusions

This study aimed to develop a set of wind assessment methods for site analysis, specifically for concave terrain conditions in coastal areas. The methods proposed here include CFD wind modelling, GIS spatial analysis, introduction of a quantifiable indicator for East Asia, establishment of wind suitability as a measure to assess wind environments in coastal concave terrains, analysis of distribution rules according to terrain features, and classification of sites based on wind suitability results.

We consider the set of methods for assessing wind conditions to be a major contribution to the process of planning and design in a residential project. With actual data from local weather stations and GIS, planners and designers can apply the methods in their decision making in the early design stages along with other considerations, such as costs, transport, and other important factors, to achieve the best land use.

Based on a total of 20 cases of typical coastal concave terrain conditions, the following conclusion can be drawn:

1. Comparative results of the average wind suitability of different sites (Fig. 12) were as follows: windward>up-crosswind=down-crosswind>leeward >crisscross. In conclusion, we recommend the selection of residential building sites with bay openings facing the direction of the prevailing wind and that the opposite direction should be avoided.

2. Correlation analysis suggested that wind suitability is significantly correlated with terrain factors. The correlation between wind suitability and altitude was the most significant, followed by the slope gradient. There was no strong association between slope direction and wind suitability.

3. Guidelines for the wind environment were proposed based on the distribution rules of measuring points of the wind field. In types I, II, III, we suggested choosing areas where the altitude was 0–10 m and the slope gradient was 20°–30°, and for types IV and V, areas where the altitude was 40–50 m and the slope gradient 30°–40°. When it came to direction, site selection varied among the different types. Overall, in types I, II, and III, it was better to use areas where the slope direction was 90°–180°, while in types IV and V, 225°–315° was recommended.

4. Formulas to estimate probabilities of preferable and undesirable wind conditions were introduced, to give a broad evaluation of wind environments. However, if detailed results are needed, we suggest using the evaluation model for wind suitability.

The study applied the general wind direction for a mesoscale region in the simulation. It did not include local winds, such as valley winds, driven by uneven heat exchange on various sides, and shore breezes due to thermal mass differences between the land and sea. A further study will include these factors to make the simulation more realistic.

Normally, thermal forces include not only wind but also solar exposure. However, this was not included in this study. This should be included in future studies to further develop the assessment system reported here. When the solar aspect is included, this method could be applied to a real planning project and help decision making by providing quantitative assessments. The planning method should be reviewed after it is implemented and realized.

References

Bowen, A.J., Hong, C., 1992. The measurement and interpretation of peak-gust wind-speeds over an isolated hill. *Journal of Wind Engineering & Industrial Aerodynamics*, **41**(1-3):381-392. http://dx.doi.org/10.1016/0167-6105(92)90436-E

Bullard, J.E., Wiggs, G.F.S., Nash, D.J., 2000. Experimental study of wind directional variability in the vicinity of a model valley. *Geomorphology*, **35**(1-2):127-143. http://dx.doi.org/10.1016/S0169-555X(00)00033-7

Castro, F.A., Palma, J.M.L.M., Lopes, A.S., 2003. Simulation of the Askervein Flow. Part 1: Reynolds Averaged Navier-Stokes equations ($k\in$turbulence model). *Boundary-Layer Meteorology*, **107**(3):501-530. http://dx.doi.org/10.1023/A:1022818327584

Cheng, X.L., Fei, H.U., 2006. The study of grid formation on complex terrain. *Chinese Journal of Computational Mechanics*, **23**(3):313-316 (in Chinese).

Chock, G.Y.K., Cochran, L., 2005. Modeling of topographic wind speed effects in Hawaii. *Journal of Wind Engineering*, **93**(8):623-638.

Dai, N., Miura, O., 1997. Soil disturbance regime in relation to micro-scale landforms and its effects on vegetation structure in a hilly area in Japan. *Plant Ecology*, **133**(2): 191-200.

Hu, C.H., Wang, F., 2005. Using a CFD approach for the study of street-level winds in a built-up area. *Building & Environment*, **40**(5):617-631. http://dx.doi.org/10.1016/j.buildenv.2004.08.016

Kubota, T., Miura, M., Tominaga, Y., *et al*., 2008. Wind tunnel tests on the relationship between building density and pedestrian-level wind velocity: development of guidelines for realizing acceptable wind environment in residential neighborhoods. *Building & Environment*, **43**(10): 1699-1708. http://dx.doi.org/10.1016/j.buildenv.2007.10.015

Kumar, S., Bansal, V.K., 2016. A GIS-based methodology for safe site selection of a building in a hilly region. *Frontiers of Architectural Research*, **5**(1):39-51. http://dx.doi.org/10.1016/j.foar.2016.01.001

Latinopoulos, D., Kechagia, K., 2015. A GIS-based multi-criteria evaluation for wind farm site selection. A regional scale application in Greece. *Renewable Energy*, **78**:550-560. http://dx.doi.org/10.1016/j.renene.2015.01.041

Launder, B.E., Sharma, B.I., 1974. Application of the energy-dissipation model of turbulence to the calculation of flow near a spinning disc. *Letters in Heat and Mass Transfer*, **1**(2):131-137. http://dx.doi.org/10.1016/0094-4548(74)90150-7

Lei, L.I., Chan, P.W., Yang, L., *et al*., 2013. Study on numerical simulation of wind field around buildings over complex terrain. *Journal of Tropical Meteorology*, **6**(10):77-81 (in Chinese).

Li, W., Wang, F., Bell, S., 2007. Simulating the sheltering effects of windbreaks in urban outdoor open space. *Journal of Wind Engineering and Industrial Aerodynamics*, **95**(7):533-549. http://dx.doi.org/10.1016/j.jweia.2006.11.001

Liu, D., Zhao, F.Y., Tang, G.F., 2010. Non-unique convection in a three-dimensional slot-vented cavity with opposed jets. *International Journal of Heat and Mass Transfer*, **53**(5-6):1044-1056. http://dx.doi.org/10.1016/j.ijheatmasstransfer.2009.11.006

Mak, M.Y., Ng, S.T., 2005. The art and science of Feng Shui—a study on architects' perception. *Building and Environment*, **40**(3):427-434. http://dx.doi.org/10.1016/j.buildenv.2004.07.016

McAuliffe, B.R., Larose, G.L., 2012. Reynolds-number and surface-modeling sensitivities for experimental simulation of flow over complex topography. *Journal of Wind Engineering & Industrial Aerodynamics*, **104-106**(3): 603-613. http://dx.doi.org/10.1016/j.jweia.2012.03.016

Meaden, G.T., Kochev, S., Kolendowicz, L., *et al*., 2007. Comparing the theoretical versions of the Beaufort scale, the T-scale and the Fujita scale. *Atmospheric Research*, **83**(2-4):446-449. http://dx.doi.org/10.1016/j.atmosres.2005.11.014

Mellor, G.L., Yamada, T., 1982. Development of a turbulent closure model for geo-physical fluid problems. *Reviews of Geophysics*, **20**(4):851-875. http://dx.doi.org/10.1029/RG020i004p00851

MHURD (Ministry of Housing and Urban-Rural Development), 2014. Evaluation Standards of Green Building, GB/T 50378-2014. National Standards of People's Republic of China (in Chinese).

Murakami, S., Deguchi, K., 1981. New criteria for wind effects on pedestrians. *Journal of Wind Engineering & Industrial Aerodynamics*, **7**(3):289-309. http://dx.doi.org/10.1016/0167-6105(81)90055-6

Murakami, S., Iwasa, Y., Morikawa, Y., 1986. Study on acceptable criteria for assessing wind environment at ground level based on residents' diaries. *Journal of Wind Engineering and Industrial Aerodynamics*, **24**(1):1-18.

Noorollahi, Y., Yousefi, H., Mohammadi, M., 2016. Multi-criteria decision support system for wind farm site selection using GIS. *Sustainable Energy Technologies and Assessments*, **13**:38-50. http://dx.doi.org/10.1016/j.seta.2015.11.007

Penwarden, A.D., 1973. Acceptable wind speeds in towns. *Building Science*, **8**(3):259-267. http://dx.doi.org/10.1016/0007-3628(73)90008-X

Ramponi, R., Blocken, B., Coo, L.B.D., *et al*., 2015. CFD simulation of outdoor ventilation of generic urban configurations with different urban densities and equal and unequal street widths. *Building and Environment*, **92**: 152-166. http://dx.doi.org/10.1016/j.buildenv.2015.04.018

Simiu, E., Scanlan, R.H., 1978. Wind Effects on Structures: an Introduction to Wind Engineering. John Wiley, USA.

Sugimura, T., Takahashi, K., Iida, M., 2009. Numerical wind analysis on complex topography using multiscale simulation model. The seventh International Conference on

Urban Climate.

Szűcs, Á., 2013. Wind comfort in a public urban space–case study within Dublin Docklands. *Frontiers of Architectural Research*, **2**(1):50-66. http://dx.doi.org/10.1016/j.foar.2012.12.002

Takahashi, T., Ohtsu, T., Yassin, M.F., *et al*., 2002. Turbulence characteristics of wind over a hill with a rough surface. *Journal of Wind Engineering & Industrial Aerodynamics*, **90**(12-15):1697-1706. http://dx.doi.org/10.1016/S0167-6105(02)00280-5

Takahashi, T., Kato, S., Murakami, S., *et al*., 2005. Wind tunnel tests of effects of atmospheric stability on turbulent flow over a three-dimensional hill. *Journal of Wind Engineering and Industrial Aerodynamics*, **93**(2):155-169. http://dx.doi.org/10.1016/j.jweia.2004.11.003

Tamura, T., 1969. A series of micro-landform units composing valley-heads in the hills near Sendai. *Control Theory & Applications IEE Proceedings D*, **127**(4):177-187.

Tamura, T., 1983. Multiscale landform classification on study in the hills of Japan: Part III application of the multiscale landform classification system to environmental geomorphological studies in the hills. *The Science Reports of the Tohoku University*, **33**(2):79-103.

Tang, L., Nikolopoulou, M., Zhao, F.Y., *et al*., 2012. CFD modeling of the built environment in Chinese historic settlements. *Energy and Buildings*, **55**(12):601-606. http://dx.doi.org/10.1016/j.enbuild.2012.09.025

Taylor, P.A., Walmsley, J.L., Salmon, J.R., 1986. Guidelines and models for estimating wind speeds at WECS sites in complex terrain. Proceedings of the Ninth Biennial Congress of the International Solar Energy Society, **4**:2009-2014. http://dx.doi.org/10.1016/B978-0-08-033177-5.50378-1

Vuorinen, V., Chaudhari, A., Keskinen, J.P., 2015. Large-eddy simulation in a complex hill terrain enabled by a compact fractional step OpenFOAM® solver. *Advances in Engineering Software*, **79**:70-80. http://dx.doi.org/10.1016/j.advengsoft.2014.09.008

Weng, W., Taylor, P.A., Walmsley, J.J., 2000. Guidelines for airflow over complex terrain: model developments. *Journal of Wind Engineering & Industrial Aerodynamics*, **86**(2-3):169-186. http://dx.doi.org/10.1016/S0167-6105(00)00009-X

Wise, A.F.E., Richards, D.J.W., 1971. Effects due to groups of buildings. *Philosophical Transactions of the Royal Society A: Mathematical Physical and Engineering Sciences*, **269**(1199):469-485.

Yan, B.W., Li, Q.S., 2016. Coupled on-site measurement/CFD based approach for high-resolution wind resource assessment over complex terrains. *Energy Conversion and Management*, **117**:351-366. http://dx.doi.org/10.1016/j.enconman.2016.02.076

中文概要

题　目：CFD 模拟下基于风适宜度的沿海岙型地形选址分析—以东亚为例

目　的：风环境直接影响居住建筑室内外自然通风、舒适度以及污染物扩散情况。本文以居住建筑选址分析为目的，建立一系列针对东亚沿海岙型地形的风环境评价方法，分析影响风环境特点的主要因素，提出风适宜度评价模型，探讨风环境与主要地形因子之间的相关性。

创新点：1. 建立东亚沿海典型岙型地形的分类数据库；2. 提出基于选址分析的风适宜度模型；3. 建立风适宜度与地形因子之间的回归模型。

方　法：1. 通过 CFD 模拟的方法，计算典型工况下 20 种岙型地形的风场（图 5）；2. 通过理论分析和数理耦合的方法，构建风适宜度模型（公式（4））；3. 通过 Logistic 回归方法，分析风适宜度与地形因子的相关性。

结　论：1. 风适宜度直接受地形特征影响，开口面向来风向的岙型地形中风适宜度平均值最高，选址过程中应避开开口背向来风向的岙型地形；2. 通过多元回归分析得出风适宜度和地形因子的相关性显著，其中海拔是决定风适宜度的主要地形因子。

关键词：风适宜度；居住建筑；CFD；沿海岙型地形；东亚